Chapter 16

Polarimetric Radar Systems

Up to this point we have seen how we can use the basic principle of transmitting a burst of energy and receiving power reflected back to the instrument in order to determine characteristics of an object or surface under study, including its location, velocity, size or composition. In all of the examples we have seen, the radar configuration consists of a single transmitting antenna and a single receiving antenna, which may or may not be co-located. We now move to systems with multiple antennas, where we can exploit different antenna properties of imaging geometries in addition to the basic observables we have to date considered.

If we use more than one antenna where each has a different polarization sensitivity, we can characterize the polarization properties of a radar echo. If we change the geometry by using two or more antennas, we will be sensitive to details of the target shape or change in shape. We will denote systems satisfying the former as polarimetric radars, or polarimeters, and the latter as interferometers. In both cases we generate additional observables by combining the signals received at two or more radar antennas.

16.1 Polarimetric Radars

We have seen that frequency diversity allows us to obtain different views of the surface through sensitivity to different size scale scatterers that are present on the surface. Now let's consider how the radar echoes are modified in polarization by interaction with the surface.

We'll call a radar with polarization discrimination capability a polarimeter, and if it produces images, an imaging radar polarimeter. We will find that different surface types cause the polarimetric signature of the echoes to have very different characteristics. First, we'll define

some basic polarization terms.

16.2 Polarization definitions

Consider this plane wave solution to Maxwell's equation:

$$\underline{E} = Re\left[(E_h\hat{\mathrm{h}} + E_v\hat{\mathrm{v}})e^{-j(wt-kz)}\right] \tag{16.1}$$

where $\hat{\mathrm{h}}$ and $\hat{\mathrm{v}}$ are linear, orthogonal basis polarization directions. We could have used any basis, though. The linear basis convention we select here has the advantage of being readily relatable to horizontal and vertical structures on the surface, such as tree trunks (vertical) vs. randomly oriented branches (which will be at some combination of horizontal and vertical.) Here E_h and E_v are complex field amplitudes given by

$$\begin{aligned} E_h &= a_h e^{-j\phi h} \\ E_v &= a_v e^{-j\phi v} \end{aligned}$$

where a_h and a_v are positive amplitudes in the $\hat{h}$ and $\hat{v}$ directions are the ϕ's are phases. Any wave can be represented by vector

$$\underline{E} = \begin{pmatrix} E_h \\ E_v \end{pmatrix} \tag{16.2}$$

Our plane wave solution is the real part of the phasor of eq. 16.1, which we can rewrite as

$$a\cos(\phi + wt - kz) = Re\left[(a_h e^{-j\phi h}\ \hat{\mathrm{h}} + a_v e^{-j\phi v}\ \hat{\mathrm{v}})e^{-j(wt-kz)}\right] \tag{16.3}$$

To recognize this as a parametric definition of an ellipse, we express the real solution in terms of in its components in the $\hat{h}$ and $\hat{v}$ directions:

$$\begin{aligned} A_h &= a_h\cos(\phi_h + wt - kz) \\ A_v &= a_v\cos(\phi_v + wt - kz) \\ A_z &= 0 \end{aligned} \tag{16.4}$$

Eliminating the variable part of the phase follows if we rewrite eq. 16.4 using the trigonometric

sum formula:

$$\begin{aligned} \frac{A_h}{a_h} &= \cos(\phi_h)\cos(wt-kz) - \sin(\phi_h)\sin(wt-kz) \\ \frac{A_v}{a_v} &= \cos(\phi_v)\cos(wt-kz) - \sin(\phi_v)\sin(wt-kz) \end{aligned} \tag{16.5}$$

which leads to

$$\begin{aligned} \frac{A_h}{a_h}\sin\phi_h - \frac{A_v}{a_v}\sin\phi_v &= \cos(wt-kz)\sin(\phi_v-\phi_h) \\ \frac{A_h}{a_h}\cos\phi_h - \frac{A_v}{a_v}\cos\phi_v &= \sin(wt-kz)\sin(\phi_v-\phi_h) \end{aligned} \tag{16.6}$$

If we square and add the two equations 16.6 we now have

$$\left(\frac{A_h}{a_h}\right)^2 + \left(\frac{A_v}{a_v}\right)^2 - 2\,\frac{A_h}{a_h}\,\frac{A_v}{a_v}\,\cos(\phi_v-\phi_h) = \sin^2(\phi_v-\phi_h) \tag{16.7}$$

We recognize eq. 16.7 as the parametric description of an ellipse, leading to a geometric interpretation of polarization. Most authors make use of a set of auxiliary angles defined by

$$\begin{aligned} \tan\alpha &= \frac{a_v}{a_h} \\ \tan 2\psi &= (\tan 2\alpha)\cos(\phi_v-\phi_h) \\ \sin 2\chi &= (\sin 2\alpha)\sin(\phi_v-\phi_h) \end{aligned}$$

leading to a picture of the elliptical path followed by the end point of the vector ($x = A_h$, $y = A_v$) of the polarized wave as it propagates in the z-direction as in fig. 16.1. If the ellipse collapses to a line, that is $\chi \to 0$, then the polarization is called linear with orientation ψ. $\psi = 0$ is horizontal polarization, $\psi = 90^\circ$ is vertical. If $a_h = a_v$ or $\chi = 45^\circ$, the polarization is called circular. Depending on the direction of rotation the circular polarization is right-handed or left-handed.

Not only waves, but antennas exhibit polarization states that can be defined either in terms of complex amplitudes or geometrical parameters χ, ψ. Thus we can represent the polarization

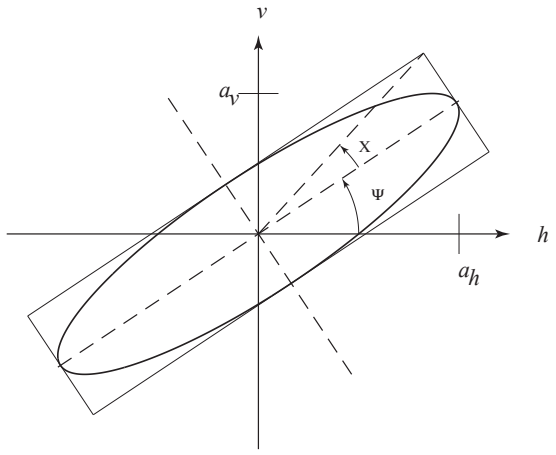

Figure 16.1: Polarization ellipse. Ellipse describes the path of a single frequency electric field vector in plane perpendicular to the wave vector. Three parameters, orientation, ψ, the ratio of semimajor to semiminor axis, or axial ratio, $\tan\chi$, and size usually of semimajor axis, a describe the ellipse. In addition a fourth parameter is required to specify the sense of rotation, either right- or left-hand (RCP or LCP); the direction of rotation is coded in the sign of χ. Altogether three numbers or parameters are required.

effects of scattering by a surface S as:

$$\begin{pmatrix} E'_n \\ E'_v \end{pmatrix}^{\text{sc}} = \frac{e^{ikr}}{kr} \begin{pmatrix} Sh'h & Sh'v \\ Sv'h & Sv'v \end{pmatrix} \begin{pmatrix} E_h \\ E_v \end{pmatrix}^{\text{inc}} \tag{16.8}$$

Here sc and inc denote the scattered and incident waves, with h, v and h', v' the bases of the two waves, which may be the same. Thus the element $Sh'h$ describes the transformation of the E_{h} component to $E_{\text{h}\prime}$ during the scattering event. Others are defined similarly. The $Sx'x$ are typically complex numbers but are often real.

The relationship of χ and ϕ to polarization is expressed as the Stokes vector, which we'll define as follows (many definitions are possible depending on bases):

$$F = \begin{bmatrix} |E_h|^2 + |E_v|^2 \\ |E_h|^2 - |E_v|^2 \\ 2Re(E_h E_v^*) \\ 2lm(E_h E_v^*) \end{bmatrix} = \begin{bmatrix} I \\ Q \\ U \\ V \end{bmatrix} = \begin{bmatrix} I \\ I\cos 2\psi \cos 2\chi \\ I\sin 2\psi \cos 2\chi \\ I\sin 2\chi \end{bmatrix} \tag{16.9}$$

The Stokes vector neatly summarizes the polarization properties of the wave. Not only does

it define the h and v components of the wave, as does the wave vector (eq. 16.2), but it also tells us what fraction of the signal power is unpolarized. For a fully polarized wave, $I = \sqrt{Q^2 + U^2 + V^2}$. But if it contains energy without a defined polarization state, we denote it a partially polarized wave, and find that $I > \sqrt{Q^2 + U^2 + V^2}$.

It is instructive to look at an example. A horizontally polarized wave has $E_h = 1, E_v = 0$. What is its stokes vector F?

$$\begin{aligned} I &= |Eh|^2 = 1 \\ Q &= |Eh|^2 = 1 \\ U &= 0 \\ V &= 0 \end{aligned}$$

Here are a few other commonly seen cases.

Vertically polarized wave:

$$E = \begin{pmatrix} 0 \\ 1 \end{pmatrix}; \text{ yielding } F = \begin{bmatrix} 1 \\ 1 \\ 0 \\ 0 \end{bmatrix} \tag{16.10}$$

Right hand circular polarization:

$$RCP : E = \frac{1}{\sqrt{2}} \begin{pmatrix} 1 \\ j \end{pmatrix}; \text{ yielding } F = \begin{bmatrix} 1 \\ 0 \\ 0 \\ -1 \end{bmatrix} \tag{16.11}$$

Left hand circular polarization:

$$LCP : E = \frac{1}{\sqrt{2}} \begin{pmatrix} j \\ 1 \end{pmatrix}; \text{ yielding } F = \begin{bmatrix} 1 \\ 0 \\ 0 \\ 1 \end{bmatrix} \tag{16.12}$$

Thus any incident wave can be expressed as one of these two forms, as can any scattered wave. Our next issue is how are these waves related for various objects, that is, what is S for different scattering types? As with the surface scattering laws we discussed in the previous chapter, calculation of these can be very challenging. But for very simple forms we can create nominal scattering matrices, and these ideal cases are surprisingly effective in reproducing backscatter observed from a real surface.

Scattering Mechanism	Scattering matrix	Notes
Sphere	$\begin{bmatrix} a & 0 \\ 0 & a \end{bmatrix}$	a real, no cross-polarized return
Bragg model	$\begin{bmatrix} a & 0 \\ 0 & b \end{bmatrix}$	b > a, slightly rough surface
Real dielectric dihedral corner reflector	$\begin{bmatrix} -a & 0 \\ 0 & b \end{bmatrix}$	a > b, both real

Table 16.1: Scattering matrices for some simple mechanisms.

Now let's consider what our received wave power looks like as a function of the polarizations of the transmit and receive antennas, respectively. Thus, if we know S for a point on the ground we can determine the received power for any combination of transmit and receive polarizations.

This variation of P with polarization is called the *polarization signature*.

Consider a plot (fig. 16.2) of the polarization signature of an object where E_r and E_t are the same, plotted as a function of χ and ϕ from the polarization ellipse. This describes a sphere with S modeled using the matrix of Table 16.1. The signal is highest for $\chi = 0$ or linear polarizations and 0 for $\chi = \pm 45^\circ$, circular polarizations.

We can easily distinguish scattering mechanisms by looking at the polarization signature. For example, in Fig. 16.3, we plot the co-polarized signatures for a rough surface and for a dihedral corner reflector. Each of these is distinct and we can recognize the scattering mechanism directly from the shape of the signature.

For targets that contain a significant unpolarized part in the echo signal, we cannot use the scattering matrix approach easily because all waves are modeled as polarized, by a *scattering*

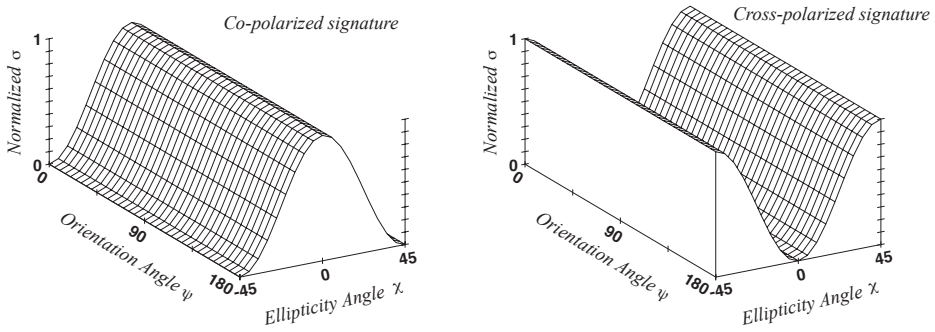

Figure 16.2: Polarization signature of sphere. At left, the co-polarized signature (transmit and receive polarizations identical.) At right, cross-polarized signature (receive polarization orthogonal to transmit polarization.) Surface represents received backscatter echo power from a sphere vs. orientation, ϕ, and ellipticity, χ.

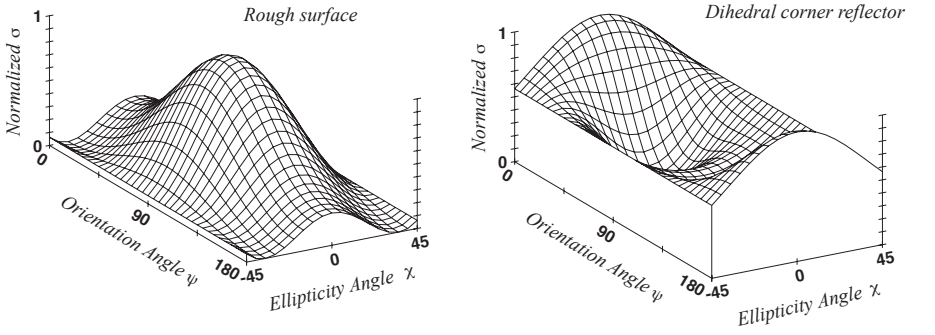

Figure 16.3: Polarization Signatures of Rough Surface and Dihedral Reflector. Co-polarized signature for a rough surface scattering according to Bragg model (left), same for a dihedral corner reflector (right). Each of these is distinct from the co-polarized sphere signature of Fig. 16.2.

matrix (eq. 16.8) of the surface. But as we saw above, the Stokes vector incorporates the randomly polarized part of wave, so we can extend the idea of a polarization signature by describing the surface in terms of a matrix relating power at distinct polarization states to a *Stokes matrix*,

$$P = F_r^T M F_t \tag{16.13}$$

where the elements of M relate the components of F_t and F_r. We can write the elements of M in terms of spatial averages of the cross products of elements of S, as in Table 16.2. Fig. 16.4 shows the co- and cross-polarization signatures from a combination of a dihedral corner reflector and a volume scattering mechanism. Here you can see the dihedral signature from

above, which sits on a pedestal of polarization-independent echo power. This type of signature is observed from some forest terrain, where the trunk/ground interaction creates a dihedral reflection, and the canopy provides a multiple scatter target. The unpolarized component often arises from such multiple scatter. The resulting polarization signature then sits on a "pedestal" of unpolarized energy.

Stokes matrix element	Definition
M(1,1)	$\frac{1}{4}[S_{hh}S_{hh}^* + S_{vv}S_{vv}^* + 2S_{hv}S_{hv}^*]$
M(1,2)	$\frac{1}{4}[S_{hh}S_{hh}^* - S_{vv}S_{vv}^*]$
M(1,3)	$\frac{1}{2}[Real(S_{hh}^*S_{hv}) + Real(S_{hv}^*S_{vv}]$
M(1,4)	$\frac{1}{2}[Imag(S_{hh}^*S_{hv}) + Imag(S_{hv}^*S_{vv}]$
M(2,1)	M(1,2)
M(2,2)	$\frac{1}{4}[S_{hh}S_{hh}^* + S_{vv}S_{vv}^* - 2S_{hv}S_{hv}^*]$
M(2,3)	$\frac{1}{2}[Real(S_{hh}^*S_{hv}) - Real(S_{hv}^*S_{vv}]$
M(2,4)	$\frac{1}{2}[Imag(S_{hh}^*S_{hv}) - Imag(S_{hv}^*S_{vv}]$
M(3,1)	M(1,3)
M(3,2)	M(2,3)
M(3,3)	$\frac{1}{2}[S_{hv}S_{hv}^* + Real(S_{hh}^*S_{vv}]$
M(3,4)	$\frac{1}{2}[Imag(S_{hh}^*S_{vv}]$
M(4,1)	M(1,4)
M(4,2)	M(2,4)
M(4,3)	M(3,4)
M(4,4)	$\frac{1}{2}[S_{hv}S_{hv}^* - Real(S_{hh}^*S_{vv}]$

Table 16.2: Stokes matrix definition.

16.3 Contrast Enhancement

Let's say we want to distinguish two different types of terrain in an image, say to make a geologic map. If we measure the polarization signature $\mathrm{P}(\chi, \phi)$ for each, we can form the ratio:

$$\frac{P_1(\chi, \phi)}{P_2(\chi, \phi)} \tag{16.14}$$

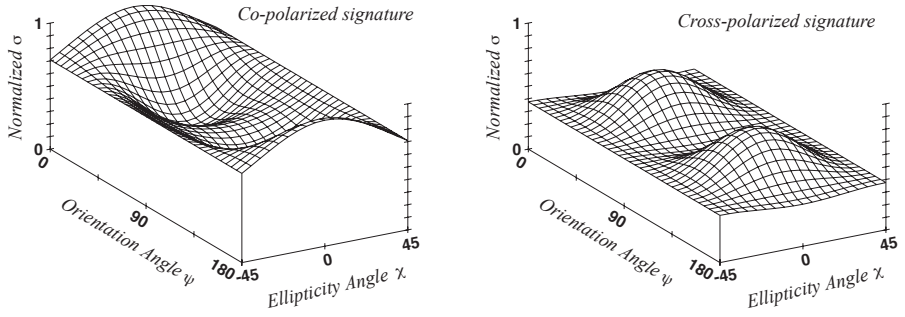

Figure 16.4: Polarization signature of a dihedral reflector plus volume scatter. For many natural surfaces, echo contains an unpolarized component in addition to any well-defined mechanism. Return from a forest, for example, might be a dihedral component from trunk/ground scattering, plus a volume term from multiple scatter in the canopy. In the presence of an unpolarized, *i.e.*, randomly polarized, component of the echo, the polarization signature appears raised by a constant power. The fraction of polarized to unpolarized echo power becomes part of the polarization signature, although the characteristics of the polarized part still largely retain their original interpretation.

and plot this quantity as a function of χ, ϕ. We could then find the maximum of this ratio, yielding the values of χ, ϕ that separates them best in the image. Generating an image with this polarization then permits the easiest mapping of those units.

16.4 Generating polarimetric data

The above applications require knowledge of S (or M) for each and every point in an image. Conversely, if we know S for each point we can implement many polarization-based analyses. So, how do we determine S observationally?

Remember S consists of the four combinations of transmit and receive polarizations (eq. 16.8.) Suppose we have two antennas on our radar, one h-pol and one v-pol. Transmit h and receive h, that measures Shh. The others follow similarly. In fact, we can transmit h and receive both h and v simultaneously in separate channels, then repeat transmitting from the v antenna. Two pulses are needed to construct the four elements of the scattering matrix.

Hence, we measure the elements of S by using two orthogonal - basis antennas, typically $\hat{\mathrm{h}}$ and $\hat{\mathrm{v}}$ but any could be used. We generate four complex radar images of each scene, one for each S element, which we can then combine to produce polarization signatures for each point

in the scene.

16.5 Unpolarized echoes

Since each measured S matrix represents a fully polarized wave, how do we estimate the depolarized part? The radar echo can be modeled as a polarized part with a distinct scattering matrix S plus a random part. Pixels spatially nearby each point on the surface might be viewed as sharing the same polarized scattering mechanism, but each with a different instantiation of the randomly polarized component of the backscatter. So if we assume the region on the surface is homogeneous, we simply spatially average the powers in the polarization signature. Note that we sum the Stokes matrices for each pixel, as these retain both the polarized and unpolarized parts of the signature in the sum. Adding scattering matrices S directly results in an average scattering matrix, which does not convey the unpolarized part of the echo. If M_i represents the Stokes matrix corresponding to scattering matrix S_i, the average Stokes matrix for all of the pixels added together results in a matrix M_{acc} containing both the polarized and unpolarized part:

$$M_{\text{acc}} = \sum M_i \tag{16.15}$$

Then the polarization signature for co-polarized antennas is $\mathrm{P}(\chi, \phi) = F_{\text{ant}} M_{\text{acc}} {F^T}_{\text{ant}}$.

We note that we can achieve the same result by computing the polarization signature for each scattering matrix pixel and then adding the signatures. The signature contains the power represented by the scattering matrix at each pixel, summing these causes the shared scattering mechanism at each point to add constructively, whereas the unpolarized, random part will vary as a function of polarization and average to a mean, nonzero value. For the coplarized signature, then, if E_{ant} is the antenna polarization (synthesized),

$$P(\chi, \phi) = \sum |E_{\text{ant}} S {E^T}_{\text{ant}}|^2 \tag{16.16}$$

This procedure is equivalent to taking looks in a conventional radar. If we store the data as a Stokes matrix in the first place, things are more straight-forward.

16.6 Example observations

As an example of what actual polarization signatures from real instruments look like, we plot in fig. 16.5 the co-polarized signatures of slightly rough surface without much vegetation and of an area in an urban setting. These data were acquired by the NASA/JPL UAVSAR airborne instrument, which operates at L-band in a small jet aircraft. By comparison with fig. 16.3, we can see that the dominant mechanisms in each case are i) the Bragg resonance model and ii) a real dielectric corner reflector formed by a building and the street, respectively. In addition to the pure mechanism suggested by the signatures, an unpolarized component is also present. This could result from any inhomogeneity in the pixels averaged to create the signature, or if there are any multiply scattered components in the return echo. The single signature shown here for each case does not allow us to distinguish these or other causes, further experiments and analyses are needed.

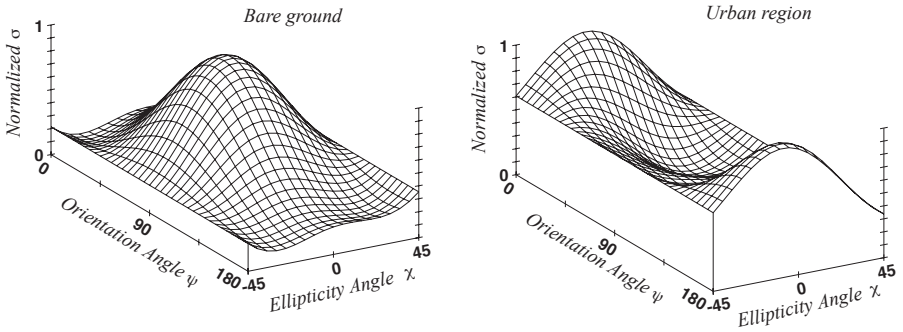

Figure 16.5: Polarization signatures of actual terrain. Measured co-polarized signatures of a patch of bare ground and of an urban area north of Los Angeles, California, as observed with the NASA/JPL UAVSAR polarimetric radar on 23 APR 2012. Note the similarity to fig. 16.3. We interpret these as identifying the Bragg mechanism as dominating for rough surfaces, and dihedral scatter as dominant in urban regions with many buildings. Note the presence of a large volume scatter component in each.

We can also use the Stokes matrices measured at every point in the image to synthesize any desired polarization transmit/receive combination. Using the Stokes matrix, we pre- and post-multiply it with the Stokes vectors for the receive and transmit polarizations, respectively, and record the measured power at each pixel to form the image. Fig. 16.6 shows four examples

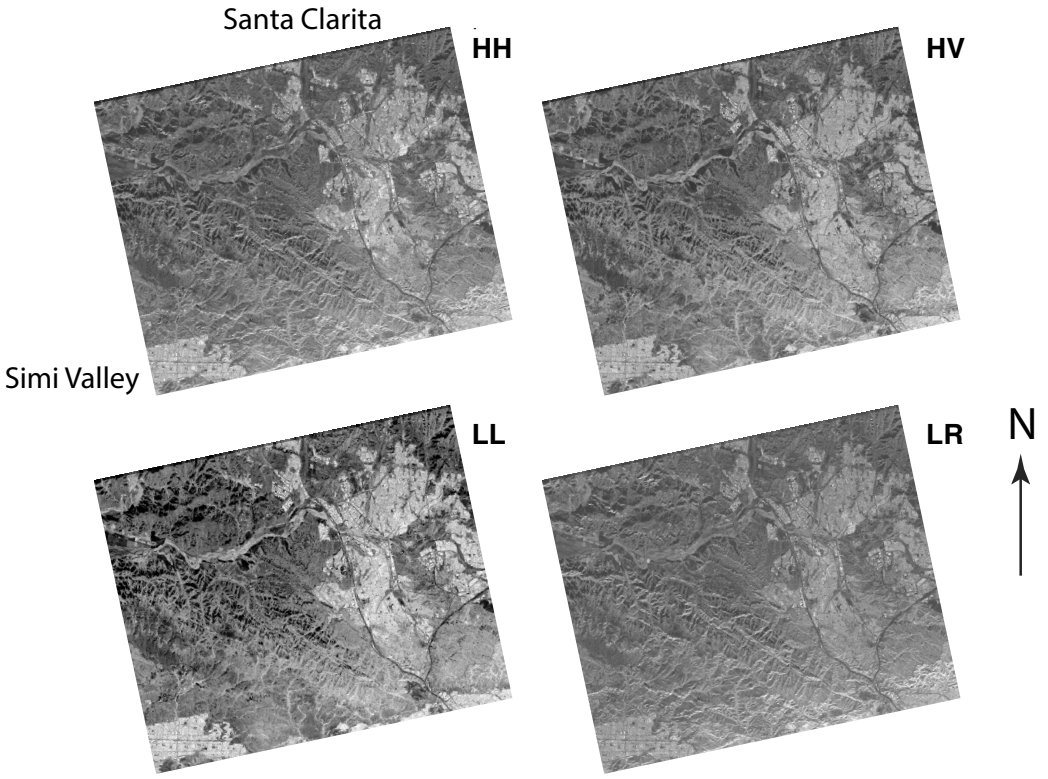

Figure 16.6: Synthesis of various polarization combinations imaging terrain. The figure displays four examples derived from the UAVSAR run used for the polarization signatures in fig. 16.5. The images, from top left in clockwise order, represent polarization pairs HH, HV, LR, LL, where H, V, L, and R are horizontal, vertical, left hand circular, and right hand circular polarizations. The first letter is the transmit polarization, the second the receive polarization.It is evident that various terrains behave differently as the the polarization is varied.

derived from the UAVSAR run described above. The images, from top left in clockwise order, represent polarization pairs HH, HV, LR, LL, where H, V, L, and R are horizontal, vertical, left hand circular, and right hand circular polarizations. These images show how differing terrains behave differently as the the polarization is varied. Depending on what ground feature is to be modeled or analyzed, descriptive polarization states may be chosen. It would also be possible to estimate the amount of the radar echo that would be considered depolarized, which may be related to how much volume scattering may be occurring in different parts of the image.